

## Article

# Adobe Blocks Reinforced with Vegetal Fibres: Mechanical and Thermal Characterisation

Angelica Rocco <sup>1,\*</sup> , Romeu Vicente <sup>2,\*</sup> , Hugo Rodrigues <sup>2</sup>  and Victor Ferreira <sup>2</sup> 

<sup>1</sup> DiArc—Department of Architecture, University of Naples Federico II, 80134 Naples, Italy

<sup>2</sup> RISCO—Risks and Sustainability in Construction, Civil Engineering Department, University of Aveiro, 3810-193 Aveiro, Portugal; hrodrigues@ua.pt (H.R.); victorf@ua.pt (V.F.)

\* Correspondence: angelica.rocco@unina.it (A.R.); romvic@ua.pt (R.V.)

**Abstract:** The present study is based on the characterisation of adobe blocks of the central region of Portugal. It is recognised that the safeguarding of the existing building stock of constructions in the traditional adobe construction technique, through different levels interventions, should also preserve the historical and cultural identity of the area as well as the traditional construction techniques, starting from the ground itself. Soil, as a repository of valuable information on the history of the site, underpins the conservation and preservation process. However, the soil is a local expression of the site, and a precise knowledge of its characteristics is necessary to hypothesise building recovery strategies. For this reason, the characteristics of adobe blocks from old buildings in the village of Torres in Anadia, in a rural area that has not yet been the subject of scientific research, were evaluated. These adobe blocks were taken from the buildings to be used in the laboratory to determine the similar mixing rates for the new adobe mixtures by analysing the material's chemical, physical, mechanical, and thermal properties, as well as its particle size distribution. In the study area, a wetland was identified characterised by a notable presence of vegetation, namely bunho and junco (*Schoenoplectus lacustris* L.). These fibres, which can be assimilated to Typha, are wild aquatic plants that can impair the biodiversity of wetlands but which, used as reinforcement for the production of adobe bricks, can stimulate new, more sustainable forms of economy in the area, which is classified as rural. The fibres were divided into two groups of 10–30 mm and 30–60 mm in length, and compositions with an additional 1 to 3% of fibres were formulated. This experimental approach was useful for understanding how the length and quantity of these fibres influence the performance of the material, thus contributing to improving knowledge about the behaviour of adobe blocks in relation to the incorporation of vegetable fibre reinforcement. The research findings reveal that the length of the fibres and percentage of incorporation have a significant impact on the mechanical behavior of the material, particularly in relation to its compressive strength up to 50%. The tested formulations were also assessed with respect to capillarity, for which most of the formulations were classified as weakly capillary, with a capillary index (Cb) of less than 20. With respect to thermal conductivity, the incorporation of fibres led to a reduction of up to 20%. The characterisations demonstrate that the optimisation of adobe is the initial stage in attaining comprehensive insight into the heritage of traditional construction in the central region of Portugal, with a particular focus on the village of Torres and the ancient adobe construction technique.

**Keywords:** adobe; vegetal fibres; safeguarding of heritage buildings



**Citation:** Rocco, A.; Vicente, R.; Rodrigues, H.; Ferreira, V. Adobe Blocks Reinforced with Vegetal Fibres: Mechanical and Thermal Characterisation. *Buildings* **2024**, *14*, 2582. <https://doi.org/10.3390/buildings14082582>

Academic Editors: Dongho Jeon and Md Morshed Alam

Received: 18 June 2024

Revised: 12 August 2024

Accepted: 15 August 2024

Published: 22 August 2024



**Copyright:** © 2024 by the authors. Licensee MDPI, Basel, Switzerland. This article is an open access article distributed under the terms and conditions of the Creative Commons Attribution (CC BY) license (<https://creativecommons.org/licenses/by/4.0/>).

## 1. Introduction

Traditional building materials have been widely used since the industrial revolution due to their durability. An analysis conducted by the International Energy Agency [1,2] revealed that these materials accounted for 30% of global final energy consumption and 27% of total energy sector emissions.

The increasing attention towards construction focuses on environmentally friendly solutions that have minimal impact on the environment and has led to the revival of traditional materials like raw earth, aligning with the principles of sustainable life-cycle strategies [3–5]. In fact, the earth gives architecture a less energy-intensive and more environmentally friendly life cycle: compared to baked clay blocks, adobe blocks, made from 15% clay, 10–30% silt, and 55–75% sand, represent a form of energy saving [6].

The earth is the foundation of the architecture that has helped to shape the landscape over the millennia: the process of soil formation is a reliable testimony to human activity, environmental factors, and the impact of different types of vegetation [7].

According to Vitruvius, in the *De Architectura libri decem*, soil could be used as a building material if it was “cretaceous” and contained a large amount of clay [8], and, following his recommendations, the ancient Romans mixed sand with clay to reduce the clay content and the risk of shrinkage during drying, added plant fibres to increase the tensile strength of the material and to regulate the water content, thus reducing hygrometric shrinkage. Finally, again in Vitruvius’ writings, it was recommended that earthen blocks be made in spring or fall to avoid excessive drying due to strong sunlight, which could accentuate the cracking phenomenon [9].

An initial visual assessment helps to understand the suitability of the soil for the use of building materials: a colour range from yellow to white indicates a predominance of sand and silt; light brown tones indicate a high clay content and/or minimal organic content; darker tones may indicate a composition unsuitable for building purposes due to a high clay content [10].

Raw earth materials, with their low environmental impact, enhance living comfort by regulating humidity through their hygrothermal properties, managing temperature, and delivering acoustic insulation [11–13].

In Mediterranean regions, with notable thermal variation during the day, earth-based constructions’ high thermal inertia due to their mass facilitates natural cooling during night hours, as remarked by Silva [14]. These materials’ acoustic insulation is significant as they are intrinsically “elastic”, able to absorb and weaken noise transmission. They serve as shields against electromagnetic contamination: a layer of earth that is 15 cm thick can reduce up to 99% of electromagnetic waves, performing better than other building materials [15]. Also in the Mediterranean area, for example, the characterisation of adobe bricks reinforced with *Posidonia Oceanica* algae has been dealt with recently, especially improving their mechanical properties due to the length of the fibres [16].

There are certain aspects of adobe that may compromise its durability. Specifically, in conditions of high atmospheric humidity, its limited mechanical resistance can lead to the occurrence of decay and disfigurement phenomena [17]. Furthermore, abrasion phenomena can lead to the development of cracks, which can then lead to saline efflorescence. In addition, it is possible that weeds or insect infestations may occur on the facade [18]. The seismic vulnerability of this type of construction should also be an aspect to be considered in the analysis [19].

During an intervention on adobe masonry, it is typical to use materials like cement or lime to preserve or restore the structure. The use of Portland cement can treat the degradation of the material by retaining water [20]. Therefore, it is recommended to prefer lime over other binders, as it fosters moisture transpiration, durability, and the resistivity of the material [21]. Stabilizing the mixture with local natural fibres has proven to enhance the physical and mechanical properties, leading to exceptional outcomes in varying climatic conditions [22]. Natural fibres can reduce differential shrinkage during drying, preventing cracks in the formulations and mixtures, improving the water repellency and cohesion of the composites [23].

In the past, synthetic fibres such as polyethylene were also incorporated into adobe bricks. However, in the present era, organic fibres are preferred for reinforcement purposes, as they are more readily disposed of [24].

The construction method based on adobe and raw earth has commonly depended on the transmission of knowledge through generations, mainly comprising geometric concepts that focused on element dimensional proportions. Additionally, legislation has documented the geometric relationships without a comprehensive examination of the mechanical impact of the material employed. For instance, in Italy, the legislation in action is limited to the Piemonte region solely [25,26]. Several regulations and technical standards specify the minimum compressive strengths required for designing adobe walls. Various regulations and technical standards establish specific minimum compressive strengths for the design of adobe walls: the New Mexico Code indicates a compressive strength of the material (the minimum needed for the achievement of the soil walls) of  $2.7 \text{ N/mm}^2$  [27]; the Australian Standard indicates a minimum compressive strength of  $1.15 \text{ N/mm}^2$  [28]; ASTM International indicates a value of  $2.06 \text{ N/mm}^2$  [29]; the Australian standard proposes that the ideal soil for fibre stabilisation should have a liquid limit (LL) between 30% and 50% and plastic index (PI) between 15% and 35% [29]; and finally, as per Turkish regulations, raw clay bricks are required to have a minimum compressive strength of  $1 \text{ N/mm}^2$  [30].

#### *Adobe: A Heritage to Be Rediscovered and Preserved*

Earth is a highly ancient building material, dating back to the use of earth bricks in Mesopotamia about 10,000 years ago. These structures emphasise the significance of a nearby asset and its deep correlation with architecture, scenery, and the encompassing surroundings.

According to UNESCO statistics, around 20% of the constructed assets listed in the World Heritage List comprise buildings constructed using the raw earth construction technique [31]. An analysis conducted by Saxton [32] indicated that approximately one-third of the world's population currently resides in homes made with earth, from developed to developing countries. This phenomenon is attributable both to its wide and abundant availability and to its favourable thermal and acoustic performance.

In Portugal, as highlighted in research work conducted by Varum on adobe [33], there exists a longstanding tradition of construction using earth, resulting in a multitude of well-preserved buildings that embody the local identity. The earliest indication of adobe employment in the area goes as far back as between 4000 and 3000 BC, within the Alto do Outeiro vicinity in Baleizão, situated in the Beja region [34]. Especially noteworthy are the circular architectural structures characteristic of the north-western region of the country, which have been present since protohistory. These structures showcase a typological progression from the huts constructed with plant fibres and adobe, providing evidence of Indo-European housing techniques [35]. During the rule of the ancient Roman empire, rectangular housing designs were developed for non-residential buildings, sidewalks, and walls. These designs gradually replaced circular structures made from plant fibres, branches, and adobe blocks, as rectangular-shaped roofs were introduced. Within this context, the Castreja house emerged, noted by Vitruvius for its thermal properties [8].

According to information obtained from the 2021 census, the implementation of adobe as a construction technique accounts for 5.32% of the complete architectural history of Portugal. In total, 178,422 structures were built using this method, clustered in a comprehensive area stretching from south to north and primarily impacting the regions of Setúbal, Évora, Portalegre, Santarém, Leiria, Coimbra, and Aveiro [36]. Furthermore, the traditional use of taipa (also known as pisata earth), tabique (wattle and mud structures), and adobe for raw earth construction techniques can be attributed to the central and southern regions of the country [37]. Finally, in regions where there is a high availability of resistant stone for construction, the adobe technique is less expressive [38].

The earliest known instance of adobe in the Aveiro region can be traced to a rural property featuring a courtyard in Vouga-Sul, built in the 18th and 19th centuries. However, earlier precedents exist, evidenced by traces of adobe in Santa Olaia from the Bronze and Iron Ages [39]. The prevalence of adobe during the Art Nouveau movement in the first half of the 20th century was noteworthy [40,41]. The buildings' facades have a ceramic tiling to

prevent water contact, thanks to the local azulejo factories. Furthermore, since the 1960s, a reinforced concrete and adobe mixed construction technique has emerged [42].

In the city of Aveiro, approximately 20% to 25% of buildings are made of adobe, with two or three floors. Adobe is used for the foundations and exterior walls, while tabique is used for the internal partitions. The floors are made of wood, and the roofs are wooden structures covered with ceramic tiles [43,44]. The wall surfaces are plastered with an earth mortar like the basic mixture of adobe blocks, to improve the interaction between the different constituent elements [45]. To enhance soil characteristics, which are characterised by a low clay content, the application of stabilisers like aerial lime are crucial. This improves the ability of the blocks to withstand water exposure, contributing to increased durability [14] or, if unsterilised blocks are used, to the addition of vegetable fibres, predominantly straw and dried reeds [37].

The measurements of the adobe blocks within the Aveiro region have been recorded using the moulds from Quinta do Areal factory. The dimensions of the adobe blocks for adobe walls are  $0.45\text{ m} \times 0.15\text{ m} \times 0.12\text{ m}$ , whereas formats of  $0.45\text{ m} \times 0.30\text{ m} \times 0.12\text{ m}$  are appropriate for adobe structural walls. Additionally, these adobe blocks can also be used to construct curved shapes for well walls [38].

In a recent study, 41 adobe blocks collected from the central regions of Portugal underwent characterisation. Through this study, five distinct types of adobe were identified based on their visual properties, four types based on mineralogy, and three types based on their chemical composition and mechanical behaviour [37]. The analysis has indicated that the blocks consist primarily of minerals like quartz, calcite, and phyllosilicates, exhibiting mechanical strengths that range from 0.30 to 3.50 MPa. In this region, the deterioration of the adobe is attributed to water exposure and the development of cracks due to the stresses and loads on the structure. These cracks are frequently addressed by injecting and applying mortar onto the affected surface [42].

At the source of these considerations, we see the need to boost scientific research efforts, since knowledge is the basis of any future strategy aimed at safeguarding such heritage built with the adobe construction technique.

Although so many constructions fall in the central area of Portugal, the soil is characterised by its local specificity and timely knowledge is necessary. Actions aimed at preservation also can stimulate new economies in these rural areas: reinforcing adobe blocks with wild and weedy plants, a practice already established in the Mediterranean, supports the production of a low-cost building material, creating new economies in rural areas and contributing to the landscape. As other researchers have also pointed out [41,46–49] such blocks can be used both for rehabilitation operations and for the construction of new buildings, maintaining a typological–compositional linearity and providing an alternative to passive solutions.

In sum, from locally available and abundant materials, such as soil and plant fibres typical of wetlands, a low-cost material can be produced to contribute to energy retrofits of the pre-existing urban adobe building fabric for the preservation of this UNESCO-protected building technique.

## 2. Case Study

This case study involves, in a first stage, the analysis of adobe blocks obtained from a building dating to the late 19th century situated in the Aveiro district, specifically in the village of Torres, Anadia, in Portugal. Figure 1 displays the historical progression of adobe construction techniques in the area under examination, emphasising the significance of acquiring knowledge of the construction method that differentiates the urban landscape to prepare for future interventions.

The second stage of the study, based on the understanding of the material and the regional construction method, included trials to produce adobe bricks by incorporating indigenous plant fibres, *bunho* and *junco*, particular to the wetland region under analysis. This fibre closely resembles the *Typha*, a rapidly growing perennial plant found in aquatic



ecosystems, growing up to 2 m in height. A research study conducted between 1994 and 1999 on 374 fibre samples collected from Korea to Russia aimed to determine the morphological properties of the *Typha* genus, identifying four distinct species. The selection of this fibre is therefore a representative of wild plants found in humid areas [50]. In Estonia, the utilisation of *Typha latifolia* in construction has become standard practice [51]. This is due to its high concentration of polyphenols, which provide exceptional resistance to mould and bacterial infections [52]. Furthermore, it possesses a structure comprising 85% parenchymatous tissue, leaves with high porosity, and a low density of approximately  $30 \text{ kg/m}^3$ . Additionally, its thermal conductivity is lower than that of polystyrene ( $\lambda = 0.032 \text{ W/m K}$  compared to  $\lambda = 0.04 \text{ W/m K}$ ), making it a practical alternative [51].

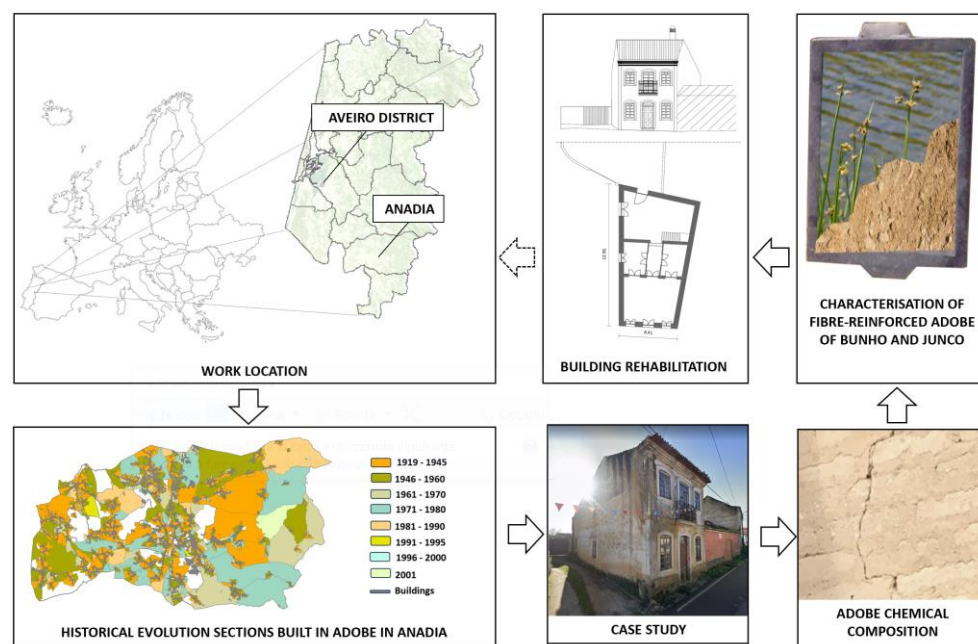


**Figure 1.** Case study in Anadia (Aveiro, PT). The characterisation of fibre-reinforced adobe will improve the redevelopment process for the case study and help preserve the heritage of Anadia's adobe buildings.

### Work Methodology

The soil composition reveals the geological history of the land. It is a vital constituent for repair and refurbishment of adobe buildings, which feature prominently on the site of the case study. A proficient comprehension of the physical, chemical, and mechanical properties is necessary to implement appropriate and effective conservation measures to mitigate degradation processes. The preservation of the building includes aspects such as structural integrity, historical-cultural significance, and its contribution to the local identity and socioeconomic development. To address the research questions, the analysis was conducted in three distinct stages as shown in Figure 2.

As a first step, a specimen of adobe was extracted from a representative building of the village of Torres and analysed by means of mineralogical and chemical assessment, compression and flexural strength tests, particle size characterisation, and thermal conductivity tests. This stage is vital to ascertain the soil properties and advance to the subsequent stage of incorporating indigenous plant fibres into the adobe.

In the second stage, a thorough experimental campaign was conducted on adobe blocks strengthened with local bunho and junco plant fibres, typical of the wetland area under study. These blocks were created using adobe with soil characteristics like those of the original adobe. Various adobe mixtures with different contents and lengths of fibres were produced. Tests were performed to determine their physical and mechanical properties.

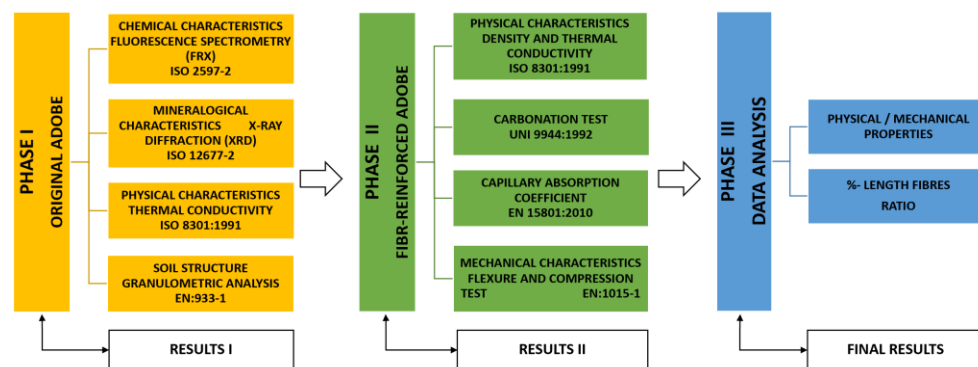


**Figure 2.** Work plan phases according to current standards [53–56] in Phase I and [55,57–59].

Finally, in phase three, the possible benefits of reinforcing plant fibres in the adobe brick mix on properties were evaluated, considering both the effects of the added percentage and the length of the fibre cut.

### 3. Materials and Method

#### 3.1. Phase I: Characterisation of Original Adobe

##### 3.1.1. X-ray Diffraction (XRD) and Fluorescence Spectrometry (FRX)

The mineralogical composition of adobe determines the plasticity of clays. Tests using X-ray fluorescence spectrometry (FRX) and X-ray diffraction (XRD) were carried out [60].

Chemical analysis via FRX was conducted to quantify the chemical elements present in the samples. The mineralogical analysis was conducted using X-ray diffraction (XRD) with the Philips X'pert-PRO MPD diffractometer, which had a PW3050/60 Ka Cu radiation goniometer.

##### 3.1.2. Assessment of Aggregate Properties

Particle size distribution was done by sieving, defining a granulometric curve used for soil classification and compared with the USCS (Unified Soil Classification System) standard. This standard identifies four classifications: gravel ( $d > 2$  mm), sand ( $2 \text{ mm} > d > 0.06$  mm), silt ( $0.06 > d > 0.002$  mm), and clay ( $d < 0.002$  mm) [61].

##### 3.1.3. Determination of the Insoluble Residue in HCl, Capillary Absorption, and Density of the Material

It is crucial to determine the insoluble residue in hydrochloric acid (HCl) in accordance with the EN 932-2:1999 [62] standard to establish the sample's purity. Following the permeability and fixed residue calculations and obtaining values stabilised below 0.1% mass, the material's density is determined (see Figure 3).



**Figure 3.** Testing of residue insoluble in HCl.

The percentage of insoluble residue  $R_i$  was then calculated according to:

$$R_i = \frac{m_r - m_0}{m_a} \times 100\%$$

where  $m_r$  is the weight of the filter containing the residue,  $m_0$  is the weight of the filter, and  $m_a$  is the weight of the sample.

The value of the absorbed capillary water by the sample per unit area is given by the following equation:

$$AC = \frac{(m_i - m_0)}{A}$$

where  $AC$  is the capillary absorption expressed in g/dm<sup>2</sup>,  $m_0$  is the initial mass of the sample before the start of the test (g),  $m_i$  is the mass of the sample weighed at each time interval (g), and  $A$  is the cross-sectional area of the sample (dm<sup>2</sup>).

The average of the variation in water content is given by the equation:

$$w = \frac{(m_t - m_s)}{m_s} * 100 (\%)$$

where  $W$  is the water content (%),  $m_t$  is the mass of the sample at a given drying time  $t$  (g), and  $m_s$  is the dry mass of the sample (g).

Finally, density [57] refers to the function:

$$\rho = \frac{M}{V}$$

where  $M$  is the mass in kg and  $V$  is the volume in m<sup>3</sup> of the tested samples.

#### 3.1.4. Particle Size Analysis

This European standard specifies a method for determining the particle size distribution of aggregates by sieving in accordance with EN 933-1:2012 [56].

The determination of the proportions of the different size fractions present in the initial samples after the disintegration process was carried out by analysing the particle size distribution under drying conditions. This process was carried out using a series of sieves with openings ranging from 0.075 to 63 mm (see Figure 4).



**Figure 4.** Insoluble residue to be subjected to particle size analysis.

#### 3.1.5. Thermal Conductivity

The thermal conductivity test was carried out on four samples measuring 400 × 400 × 40 in accordance with the ISO 8301 test method [55]. By using a device to measure the actual heat flow through the sample, it is possible to determine the thermal conductivity of the material at the average temperature established between the two plates (47.5 °C in our case) by applying the equation:

$$\lambda = \frac{Q \cdot t}{\Delta T}$$

where  $Q$  is the heat flux through the sample,  $t$  is the thickness of the sample, and  $\Delta T$  is the temperature difference between the plates (see Figure 5).

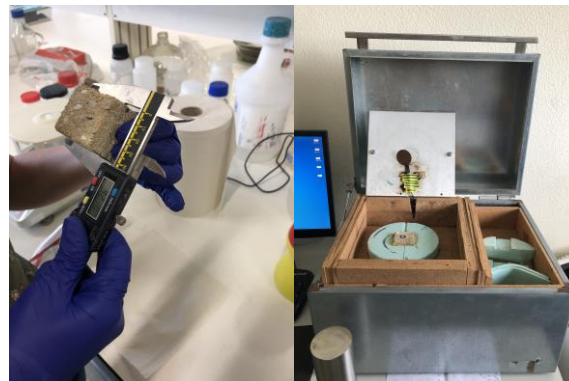


**Figure 5.** Thermal conductivity test. After each sample is measured, it is inserted into the thermal conductivity measuring equipment.

### 3.2. Phase 2: Fibre-Reinforced Adobes—Production and Characterisation

#### 3.2.1. Production of Adobe with Fibres

Earth has been used as a building material since ancient times. The experimental campaign is based on ancient Roman indications for producing adobe blocks. Vitruvius [60] suggested in his writings that earth can be used as a building material, provided that it contains a significant amount of clay. The Romans followed these guidelines and combined sand with clay to reduce the clay content and the risk of shrinkage during the drying process. Furthermore, the researchers mixed plant fibres with the material to improve its tensile strength and regulate water content, mitigating hygrometric shrinkage. They also recommended producing earth blocks during spring or autumn to avoid excessive drying caused by intense sun, which can lead to cracking [9]. Therefore, the adobe blocks used in the application case were produced in June to avoid the above-mentioned issues. Subsequently, we produced adobe blocks using a soil that closely matched the original composition. Finally, the characteristics of the adobe blocks with different amounts of vegetable fibre reinforcement were evaluated. The adobe allows the required workability of the binder (cement or lime), water, sand, and aggregate mixture to achieve mechanical, chemical, and physical benefits in the solid phase. The synergistic nature of reinforcing fibres can introduce improved properties to the base material [63].

In the conducted experiment, bunho and junco fibres were utilised instead of the more conventional straw material that is native to the Anadia wetland and, therefore, local.

The selection of cut and fibre amount percentage was influenced by relevant scientific literature in arriving at the incorporation levels herein proposed [16,52,64–67]. The fibres were segmented into 10–30 mm and 30–60 mm lengths with the intention of assessing the impact of the fibre length on the adobe block properties. (see Figure 6).

Different incorporation amounts of bunho and junco fibres for reinforcing adobe blocks were studied. Flexural and compressive strength of the adobe blocks after a 28-day curing period was evaluated, as well as their density and thermal conductivity.

Unfired earth is highly porous, which affects its mechanical properties and durability. In adobe reinforced with vegetable fibres, these fibres contribute to the masonry's shear and tensile strength. Investigating the impact of fibre amount and its length on material performance is crucial in determining the optimal material to produce based on test results [68].

The adobe blocks were produced following the ancient tradition of adobe block making for the central region of Portugal, as reported by [69] using the *adobera* form of dimensions  $13 \times 25 \times 40$  cm, with the inclusion of different lengths and percentages of vegetable fibres. The mixture was manually prepared to eliminate lime clumps, ensuring homogeneity, while adding water gradually. Consistent weight ratios were maintained, resulting in the



production of six adobe blocks, along with other samples in accordance with the proportion of added fibres to increase volume. The blocks underwent outdoor drying for 28 days (see Figure 7).



**Figure 6.** Bunho and junco fibres cut into two different lengths: 10–30 mm (on the left) and 30–60 mm (on the right).



**Figure 7.** Adobe block ( $13 \times 25 \times 40$  cm) manufacturing process. Image caption: (A) the adobe soil mixture is recreated based on the block taken from the representative building of Anadia and the plant fibres are added; (B) the dough is controlled with the hands to avoid lumps in the mixture and create a cohesive dough; (C) the mixture is transferred to the *adobera* to create the bricks; (D) by increasing the addition of fibres to the starting proportions of the mixture, the quantity increases and more blocks are obtained; and (E) after 28 days, the characterisation test phase begins.

### 3.2.2. Physical and Mechanical Characterisation

The thermal conductivity and density of each fibre-reinforced adobe composition, at varying contents and lengths, were evaluated.

The specimens used for the mechanical tests were of the standard type, with dimensions of  $40 \times 40 \times 160$  mm, and were placed in normalised steel drawers according to EN 196-1 2005 [70]. They were cured for 28 days under standard environmental conditions. Afterward, specimens were placed in a climatic chamber for 5 days in a vertical position at a constant temperature of  $20^\circ\text{C}$  and 65% RH [59] to eliminate any residual moisture (see Figure 8).





**Figure 8.** Adobe blocks before and after climate chamber exposure. Each number refers to a test specimen produced versus reinforcement in percentage and fiber length.

The mechanical strength tests were done according to EN:1015-11 [59]. The test included three samples in the dry state and three samples exposed to water contact for 24 h, with dimensions of  $100 \times 100 \times 100$  mm. Specimens were subjected to three-point flexure tests (Figure 9, left) and compressive tests (Figure 9, right).

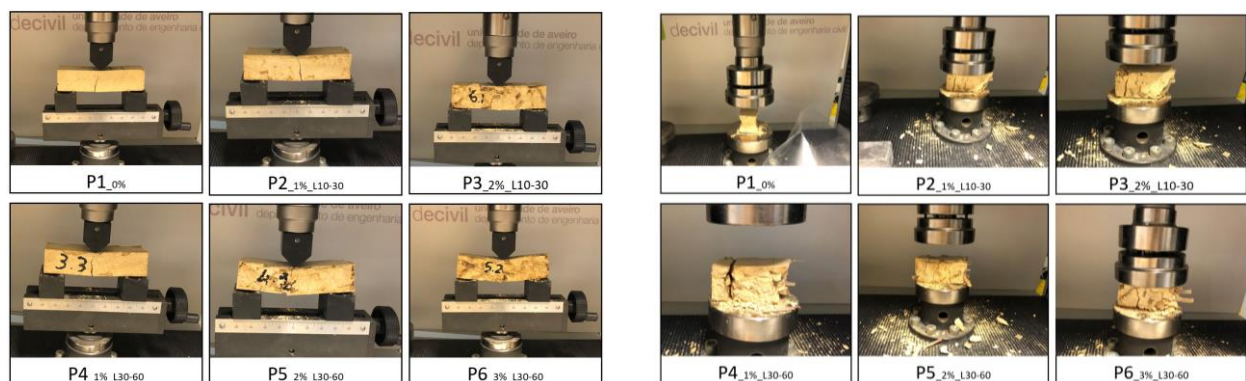


**Figure 9.** Adobe blocks: flexure test (left), compression test (right).

The mechanical compressive strength tests were performed according to EN:1015-11 [59]. The test included three samples in the dry state and three samples exposed to water contact for 24 h, with dimensions of  $100 \times 100 \times 100$  mm. These tests are essential to define the modulus of elasticity.

### 3.2.3. Carbonation Test and Capillary Absorption Coefficient

Preventing carbonation is the only way to avoid structural deterioration and consequently reduce repairing costs. The depth of carbonation can be determined by the phenolphthalein test [71]. A 1% solution of phenolphthalein in ethyl alcohol was used here. Phenolphthalein turns pink on contact with solutions with a pH above 9.2 and remains colourless at lower pHs, such as those in carbonated adobes. In fact, when phenolphthalein does not change colour, this indicates that all of the calcium hydroxide ( $\text{Ca}(\text{OH})_2$ ) has reacted with carbon dioxide ( $\text{CO}_2$ ) to form calcium carbonate ( $\text{CaCO}_3$ ), and measuring the thickness helps to understand on which side of the material the phenomenon is most pronounced.

Water absorption by capillary rise is one of the main water transport phenomena in several materials. It can cause deterioration of the material, such as the formation of efflorescence on the outside of the product due to the rising of soluble substances. The test was performed here according to EN 15801: 2010 [58] (see Figure 10), and the capillary absorption coefficient was calculated over 60 min for each sample.



Figure 10. Capillary absorption test.

#### 4. Results and Use

##### 4.1. Results for Characterization Results on Original Adobe and then Section

##### 4.1.1. X-ray Diffraction (XRD) and X-ray Fluorescence Spectrometry (FRX)

The mineralogical analysis identified several chemical elements at significantly higher concentrations, including  $\text{SiO}_2$ ,  $\text{CaO}$ ,  $\text{Al}_2\text{O}_3$ ,  $\text{K}_2\text{O}$ , and  $\text{MgO}$ . Other elements are present in percentages lower than 0.47%, namely  $\text{TiO}_2$ ,  $\text{P}_2\text{O}_5$ ,  $\text{Na}_2\text{O}$ ,  $\text{SO}_3$ ,  $\text{MnO}$ ,  $\text{Ba}$ ,  $\text{Sr}$ ,  $\text{Zr}$ ,  $\text{Rb}$ ,  $\text{Cl}$ ,  $\text{Cr}$ ,  $\text{Pb}$ ,  $\text{V}$ ,  $\text{Ni}$ ,  $\text{Zn}$ ,  $\text{Cu}$ ,  $\text{Ga}$ , and  $\text{Y}$ . The corresponding XRD pattern of the adobe sample showed quartz registering the highest peak at  $26.6^\circ$  and calcite at  $29.3^\circ$  [72] (see Figure 11).

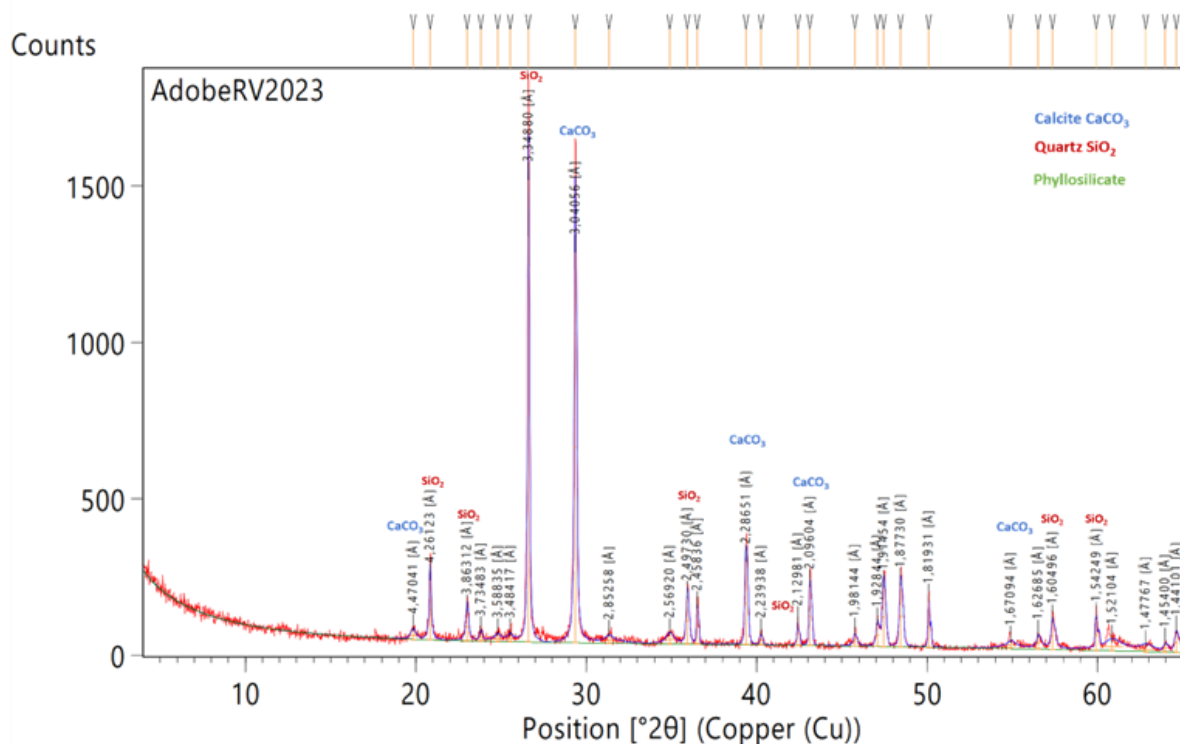
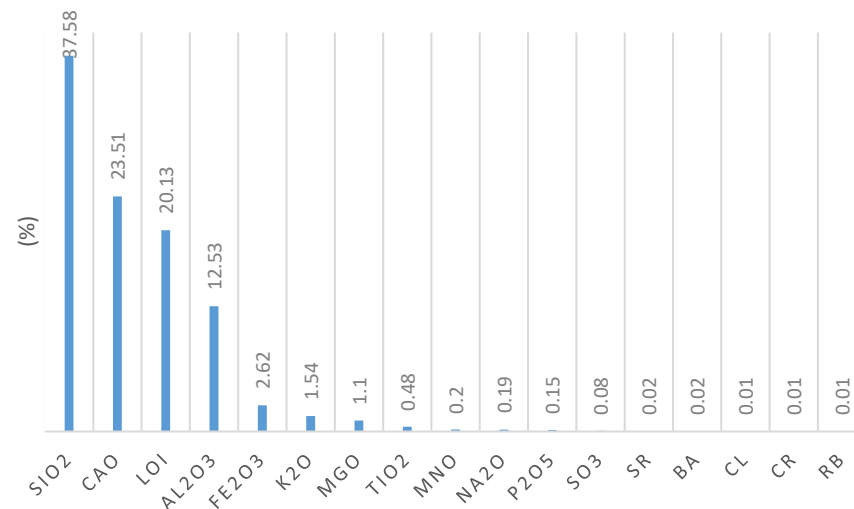


Figure 11. Soil mineralogical results. The blue lines indicate the presence of Calcite, the red lines of quazo, and the green lines of Phyllosilicate.

Quartz is present in aggregates such as sand and gravel, whereas calcite originates from the use of lime as a binder. Previous research indicates that the presence of phyllosilicates does not exceed 4% [73]. Plant fibres were not detected in the case study, although considering the brick's age of at least 100 years, the result of the mineralogical analysis's LIO may suggest a small percentage of fibres [63] (see Figure 12).



**Figure 12.** Mineralogical analysis.

#### 4.1.2. Determination of the Residue Insoluble in HCl, Capillary Absorption Density, and Conductivity of the Original Adobe

The hydrochloric acid (HCl)-insoluble residue is presented in the Table 1. These values are crucial in determining the density of the material.

**Table 1.** Hydrochloric acid (HCl)-insoluble residue \*.

Initial Weight (50 g)	m (g)	C (g)	F (g)	Double Weighing (g) m + C	Insoluble Residue (%)
ma1	m1 = 44.00	C1 = 82.85	F1 = 1.64	125.59–125.68	$R_i1 = 0.008$
ma2	m2 = 48.31	C2 = 78.34	F2 = 1.60	125.92–129.83	$R_i2 = 0.009$
ma3	m3 = 49.34	C3 = 77.59	F3 = 1.60	175.85–117.86	$R_i3 = 0.009$

\* In the test, the percentage of aggregate that remains undissolved after treatment with hydrochloric acid followed by washing with sodium carbonate solution is considered [74].

Capillary absorption is influenced by the porosity and permeability of the material, the amount of clay present, and the binder chosen.

The result of capillary absorption, calculated based on the average values of the dry and humidified adobe, is 0.178 g/dm<sup>2</sup>. The variation in percentage of the water content, calculated on the average value of the mass of the humidified sample, is 9.22%. The density is 1933.71 kg/m<sup>3</sup>, calculated on the average of the dry clay values, and 10,726.57 kg/m<sup>3</sup>, calculated on the average of the humidified clay values. The verification of the thermal conductivity of the clay gives an average value equal to  $\lambda = 0.754$  W/(mK).

#### 4.1.3. Assessment of Aggregate Properties: Granulometric Analysis

The percentage of binder is calculated from the grain size curve obtained from the adobe block taken from the building:

$$\frac{(M_i - M_m) \times 100}{M_i} = 21.2\%$$

This is an adobe based on a soil/binder ratio of 4:1. The soil is composed of sand (0.063–2 mm) at 54.96%, with the variable presence of pebbles (>20 mm), gravel (2–20 mm) at 67.44%, and silt and clay (<0.063 mm) at 2.48% (see Figure 13).

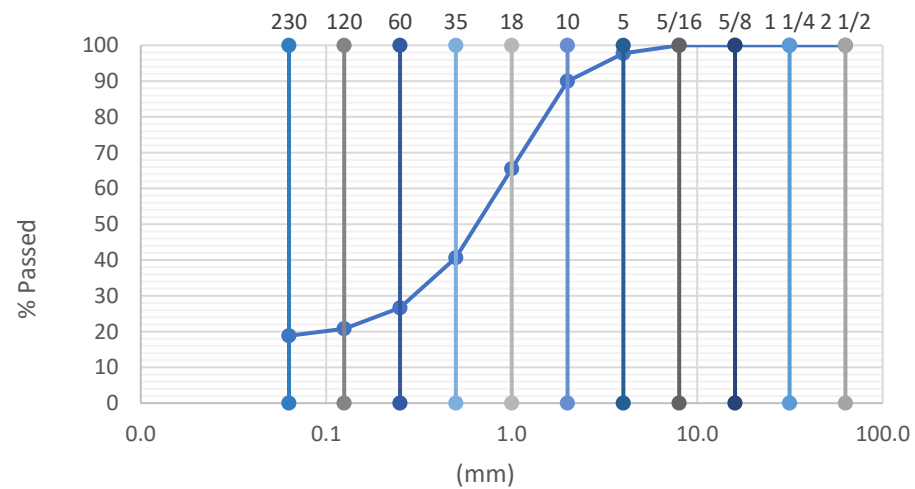


**Figure 13.** Granulometric analysis.

#### 4.2. Characterisation of Fibre-Containing Adobes

In the initial phase of the experimental work on the adobe block taken from the historic building, the grain size of two local soils was analysed, and the soil that most closely matched the grain size curve of the adobe blocks was selected. By comparing this curve with the grain size curve of the local sand, we determined the amount of silt required for the soil mixture to produce an adobe that is as representative as possible of the original composition (refer to Figure 14).

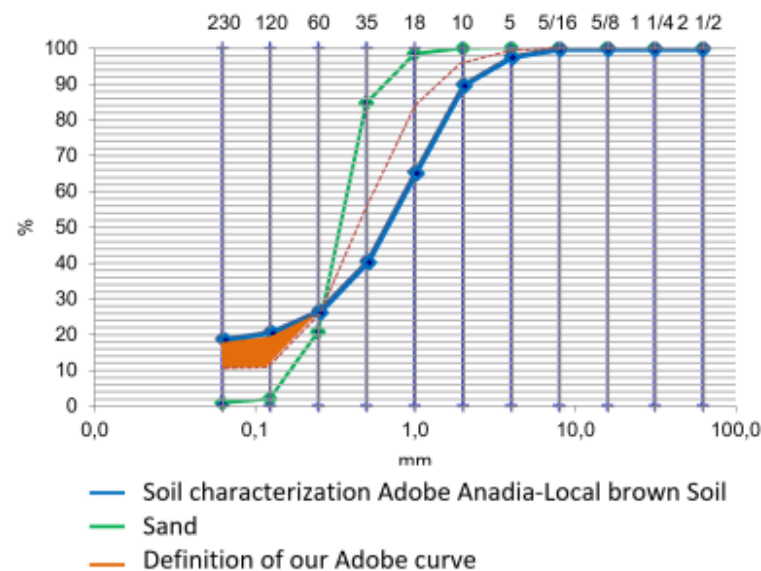


**Figure 14.** Percentage definition for adobe with fibres.

In the second phase of experimentation, adobe bricks were produced using the grain size curve results obtained in the previous phase. Bunho and junco fibres were added as reinforcement, and the blocks were cured for one year before being added dry. Given that the original block has a soil-to-water ratio of 4:1 and that adobe blocks in the central region of Portugal weighed 25 kg, optimal mixtures were achieved as shown in Table 2.

**Table 2.** Composition of adobe bricks and percentage of vegetable fibre reinforcement \*.

Adobe Specimens Ref.	Fibres %	Fibre Length [cm]	Soil [kg]	Fine Sand 0.25 $\mu$ [kg]	Binder Ca (OH) <sub>2</sub> [kg]	Ratio 4:1 (W/St) [kg]
P1 <sup>1</sup>	0	0				
P2.x_L1-3	1	1–3				
P3.x_L1-3	2	1–3	constant value:	constant value:	constant value:	constant value:
P4.x_L3-6	1	3–6	17.85	2.16	5	6
P5.x_L3-6	2	3–6				
P6.x_L3-6	3	3–6				

\* Compositions of the bricks produced: the mixture of sample P1<sup>1</sup> was recreated from the mineralogical analysis and chemical composition of the adobe brick sample taken from the case study and is the reference sample for the further samples produced with the reinforcement of plant fibres of length 10–30 mm (P2–P3) and 30–60 mm (P4–P5–P6) with 1% (P2–P4), 2% (P2–P3–P5), and 3% (P6) fibres. The ratio followed for water/soil proportions (w/s) is 4:1.

#### 4.2.1. Physical Properties: Density and Thermal Conductivity

In this study, the P6 sample achieved the lowest lower thermal conductivity. Ba et al. discovered that increasing the percentage of fibres and their length has a positive impact, promoting the growth of micropores and macropores in composites [67]. Their research revealed a range of thermal conductivities, from 0.335 to 0.113 W/m. When 30% and 55% fibres were added with cuts of 1 cm and 3 cm, respectively, the conductivity of Charai's [75] results demonstrated that in comparison to 0%, at which thermal conductivity was 0.770, when 2% fiber reinforcement was incorporated, it was reduced to 0.558, followed by a further decrease to 0.460, 0.358, and 0.333 at 4%, 6%, and 8% concentrations, respectively. Incorporating 8% PS fibres could increase adobe's thermal insulation by 56.7% and its heat capacity by 17.9%. Samples P3 and P6 return low thermal conductivity; therefore, they offer greater resistance to the passage of heat flow, making them good insulators.

The density of our adobe increases as the fibres are added, ranging from 1714 kg/m<sup>3</sup> without any addition to 1431–1445 kg/m<sup>3</sup> with 1% addition, 1542–1546 kg/m<sup>3</sup> with 2% addition, and finally 1278 kg/m<sup>3</sup> with 3% addition (see Figure 15). Our results are consistent with those of Charai [75], who found a decrease in density from 1985 to 1303 kg/m<sup>3</sup> as the fibre content increased, with density values of the tested adobe with fibre incorporation between 1806 and 1787 kg/m<sup>3</sup> for adding 2–4% fibre.

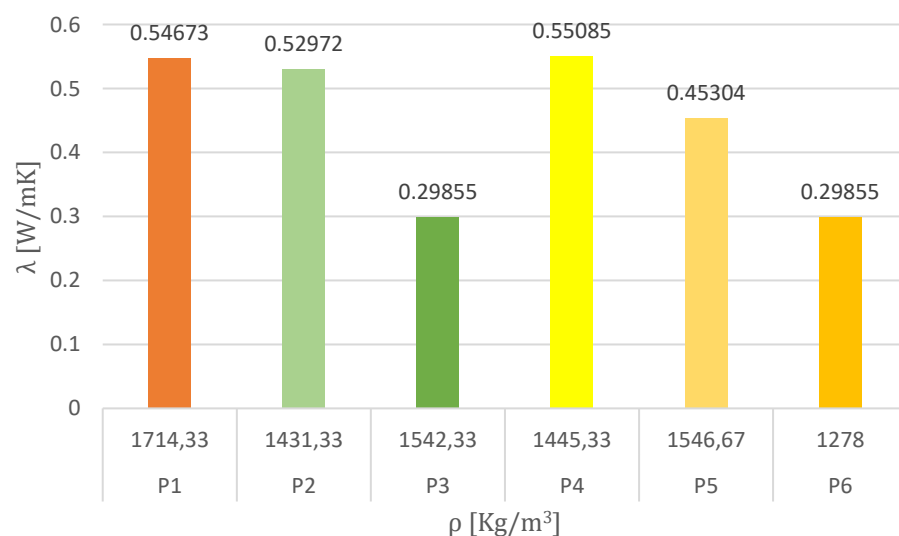


**Figure 15.** Thermal conductivity vs. density. Control volume P1 is used in conjunction with 1–3 mm long fibres in P2–3 and 3–6 mm long fibres in P4–5–6.



#### 4.2.2. Results Carbonation Test and Capillary Absorption Coefficient

The carbonation test shows that adobe blocks are not completely dry after 28 days. These tests should be repeated at least 90 days later [63] (see Figure 16).



**Figure 16.** Carbonation test.

The diagram below shows the results of the water absorption test. The best results are obtained with P2, with 1% of 10–30 mm fibres, followed by P3 and P4 with 1% and 2% of 30–60 mm fibres, P6 with 2% of 10–30 mm fibres, and finally P5 with 3% of 30–60 mm fibres. The findings demonstrate that incorporating fibres enhances the adobe's resistance against water capillarity, aligning with earlier research [47,76] which emphasises the effectiveness of adding fibres to adobe blocks to regulate moisture and thermal inertia, and contributing, as well, to living comfort. Our findings show that when fibre aggregates with a content of 6% or less are added [77], the tested formulations can be classified as weakly capillary ( $C_b < 20$ ) (see Figure 17). Manufactured blocks prove to be particularly useful in construction to reduce problems such as capillary rise, which can cause structural damage and degrade the thermal and mechanical properties of buildings.

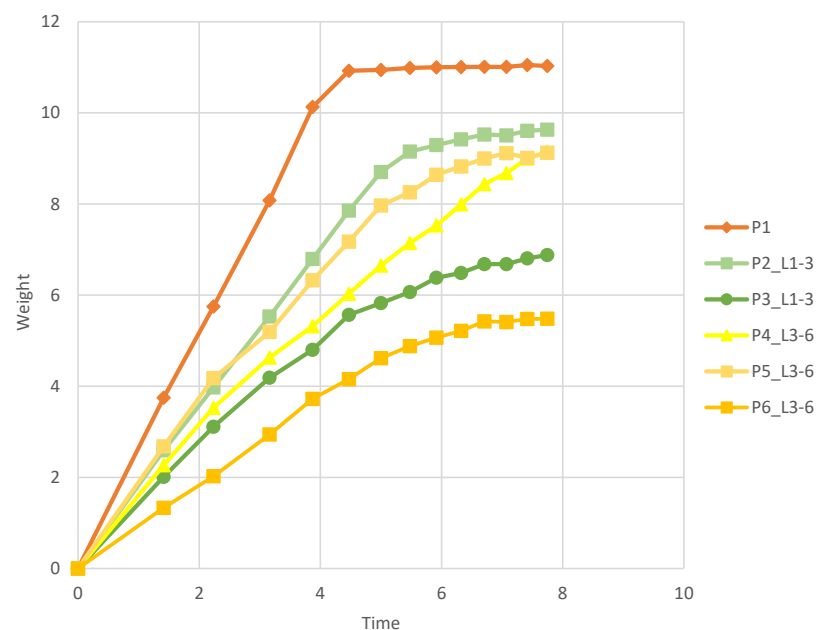


**Figure 17.** Histogram of absorption value. The weight of the samples ( $\text{g/m}^2$ ) on the y-axis versus time (seconds) on the x-axis.

#### 4.2.3. Mechanical Properties: Flexure

Mechanical flexural and compressive tests were carried out only on the fibre-reinforced adobe specimens, so a comparison with the original adobe block is not possible.

The results of the mechanical properties of the adobe samples after 28 days are shown in Table A1 in Appendix A.

The flexural test (see Figure 18) was conducted on the P1 reference adobe block without fibre reinforcement, resulting in a strength of 0.48 MPa. When 10–30 mm fibre reinforcement was added at 1 and 2%, the strength decreased to 0.40 MPa for P2 and 0.17 MPa for P3. Further reduction in resistance was observed with the reinforcement of fibres with 30–60 mm to 1.2 and 3%, resulting in strengths of 0.42 MPa for P4, 0.28 MPa for P5, and 0.16 MPa for P6. In the graph, it is shown that for the control volume P1 and for the fibre-reinforced specimens P2, P3, and P5, linear elastic behaviour is manifested up to a maximum load. The specimens P3 and P6 have a two-phase behaviour since, after the peak and rupture, there is a second phase characterised by a decrease in flexural strength, accompanied by plastic deformation with a gain in residual strength. This phenomenon has also occurred in previous research [77], and the two-phase behaviour makes the materials more resistant to seismic action and durability issues. Similarly, the addition of 30–60 mm fibres at 1–2–3% resulted in a reduction in strength to 0.42–0.33–0.17 MPa, respectively (see Figure 19).

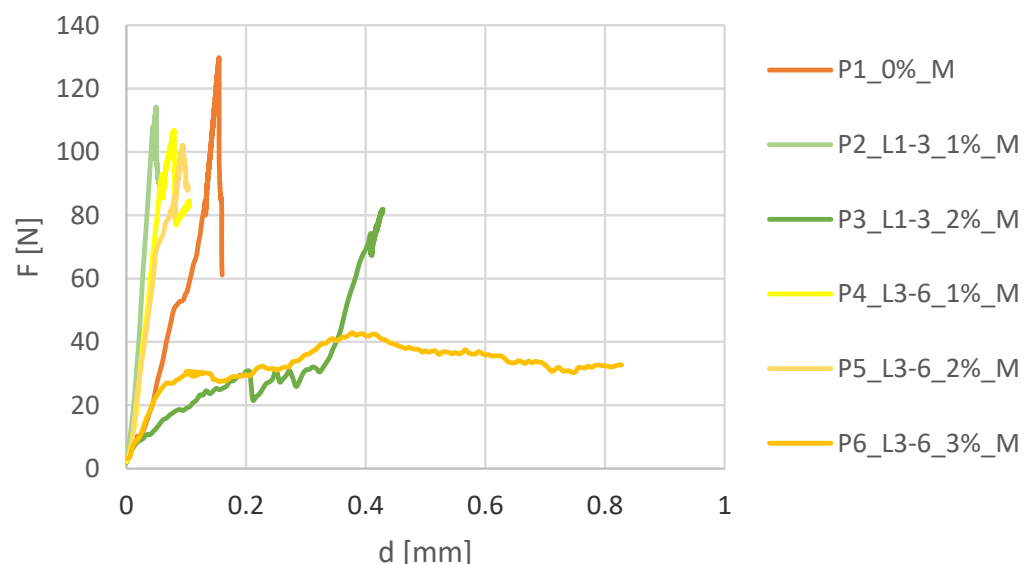


**Figure 18.** Flexural test force/displacement ( $F/d$ ) results: the bending test results are presented in the graph, which shows the average for the three species of each sample. Sample P1 did not contain any fibres, while samples P2 and P3 contained fibres ranging from 1 to 3 cm. Samples P4, P5, and P6 contained longer fibres, ranging from 3 to 6 cm. P5 and P6, despite having lower resistance, demonstrate greater durability in the curve.

These values are lower than those reported in previous studies [77], where adobe without fibre reinforcement demonstrated increased strength of 2.26 MPa. However, with the addition of 2% and 4% fibre, the strength was reduced to 1.50 MPa and 0.69 MPa, respectively. It is important to acknowledge that the comparison with the characterisation results of the materials, specifically in the case of adobe, reflects the unique local characteristics of the soil and reinforcing fibres. However, such comparisons can be useful as a reference range.

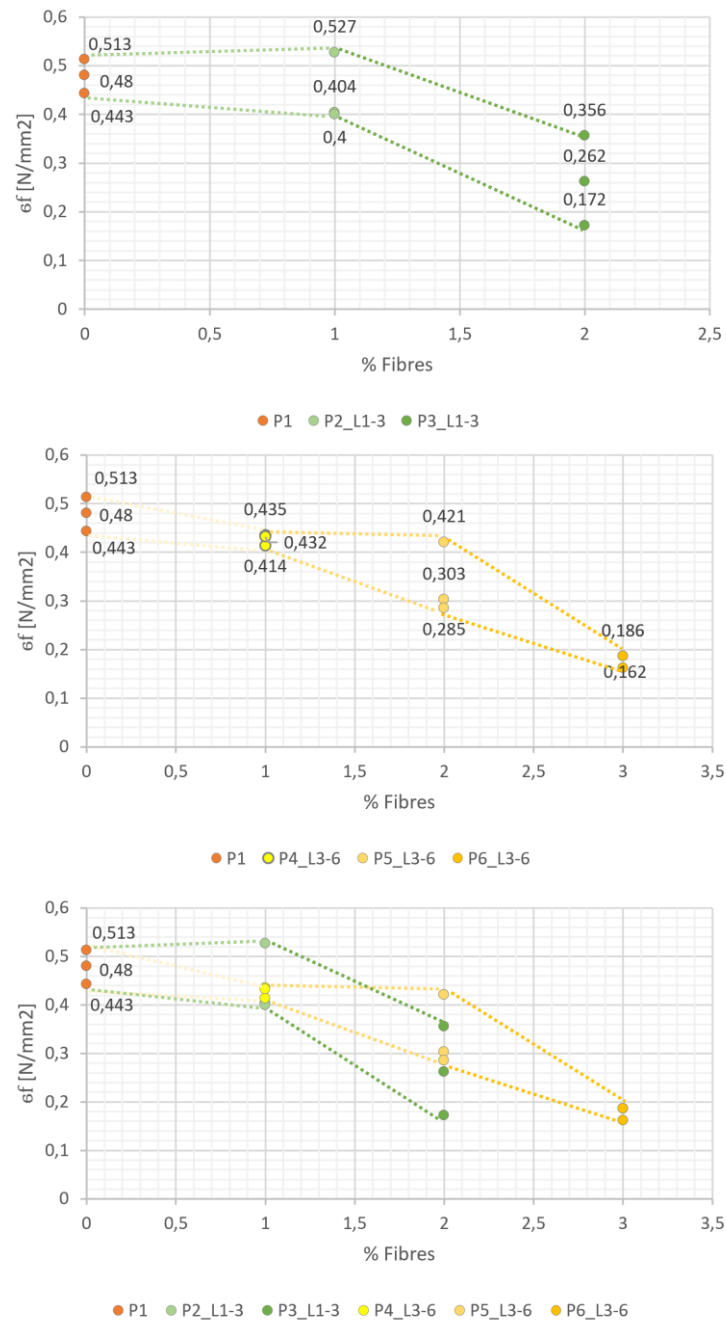


**Figure 19.** Effects of length and percentage of fibres on flexural strength (**top**: length 1–3 cm, **middle**: 3–6 cm, **bottom**: union framework).

#### 4.2.4. Mechanical Properties: Compression

The compression test was carried out on the fibre-reinforced adobe. The results showed that the maximum stress ( $\sigma_{c \max}$ ) was 1.61 Mpa and failure occurred at  $F_{\max}$  of 2.58 kN (see Figures 20 and 21).

The length of the fibres influences the results of the compression test, and it is possible to compare the adobe with 2% of 10–30 mm length with that with 1% of 30–40 mm length.

Increasing the volume fractions and fibre lengths in a composite lead to an expected impact on its mechanical properties, reducing compressive strength. This is mainly due to the increase in porosity, resulting in a decrease of the material's density. However, longer fibres can enhance the composite's tensile strength, as the flexural strength of the fibres themselves plays a crucial role in determining the material's ability to withstand tensile stresses within the matrix [67].

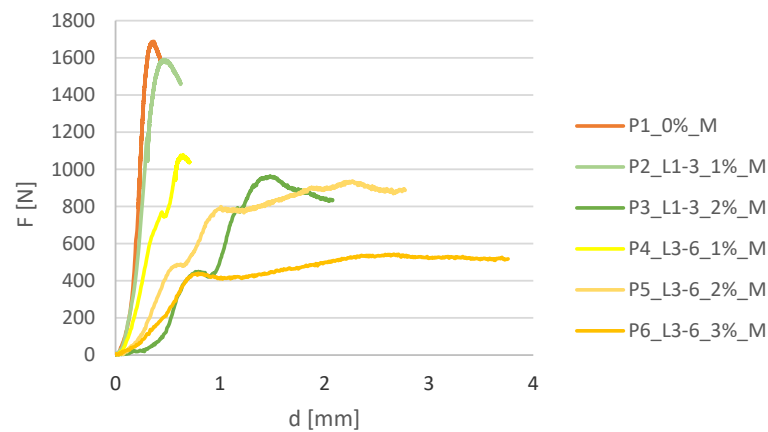


**Figure 20.** Compression test results. Force/displacement ( $F/d$ ).

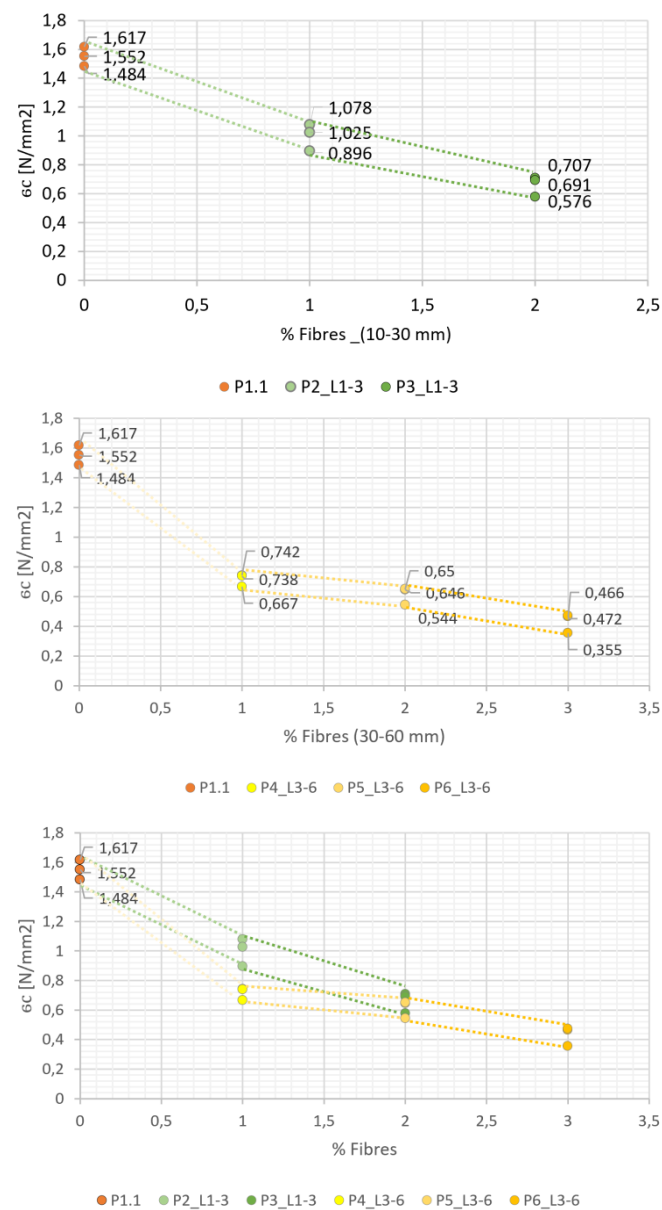


**Figure 21.** Effects of length and percentage of fibres on the compression strength (**top:** length 1–3 cm, **middle:** 3–6 cm, **bottom:** union framework).

The compressive strength of extracted adobe was 1.48 Mpa. The compression was reduced to 1 Mpa when adding 1% of fibres sized at 10–30 mm and the strength was reduced to 0.65 at 2%.

Adding 1% of fibres sized at 30–60 mm decreased the strength to 0.71, adding 2% decreased it to 0.59, and adding 3% to 0.43. The compressive strength of adobe was 1.48 Mpa. Notably, the addition of 2% fibres with the smaller size range and 1% fibres with the larger size range had an equal effect on the compression strength. Our findings align with Charai's study, in which the compressive strength of adobe decreased by up to 40% with the addition of 2% by weight of fibres, and by 55 to 59% with more than 2%. Similar findings were discovered in Khoudja et al.'s [77] on the impact of date palm fibres. With weight percentages from 0 to 10, on the thermo-mechanical properties of adobe blocks, the change from the control sample to the sample with DPW at 10% revealed a decrease in maximum strength from 6.83 to 0.55 Mpa. However, it has been demonstrated that by using the same soil and test procedures, the incorporation of palm fibres results in an increase in compressive strength, while the incorporation of pineapple fibres leads to a decrease. From here it can be understood that the choice of plant fibre to be used as reinforcement for adobe bricks is crucial because the fibre improves the quality of the material, as it itself has thermo-mechanical properties that help improve the final properties of the bricks. It is no coincidence that in various studies, the fibre is subjected to characterisation tests to understand whether it is suitable to produce building materials, and for which types of materials it is best suited.

#### 4.2.5. Elasticity Module

The stress–strain curve, based on bending test data, provides information on material toughness, indicating remarkable outcomes for P3 samples with a 2% fibre concentration at 10–30 mm. P4 samples with a 1% fibre concentration ranging from 30 to 60 mm follow closely (see Figure 22).

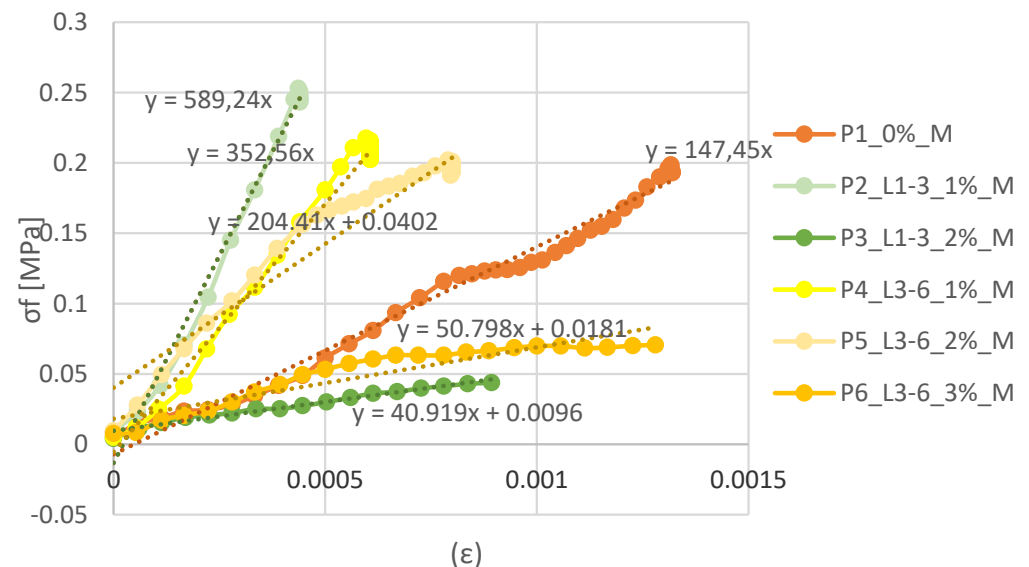


**Figure 22.** Tension–deformation of material subjected to tensile loading. The linear portion of the curve is the elastic region, and the slope of this region is the modulus of elasticity or Young's modulus.

Young's modulus, computed from compression values, offers vital insights into a material's capacity to resist compression and its rigidity when under such stress. The values remain acceptable by adding 2% fibres (see Figure 23).



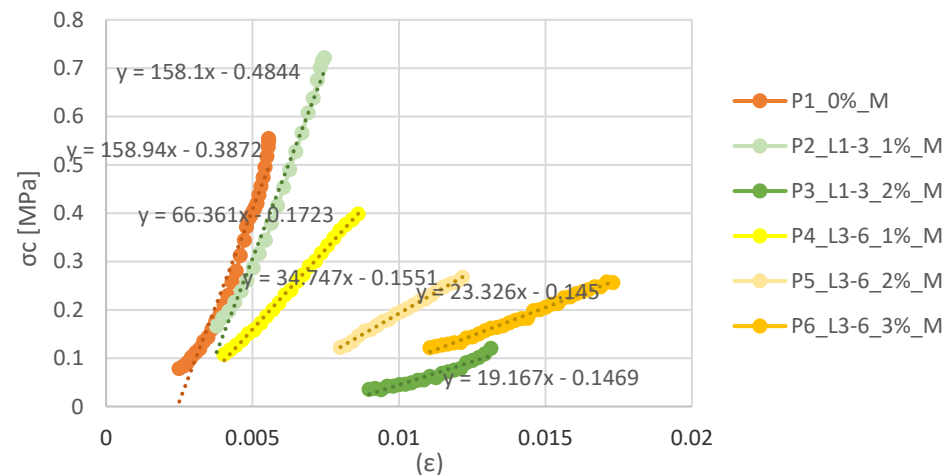


Figure 23. Compression tension–deformation of material subjected to compressive loading.

## 5. Discussion of Results

Table 3 shows the main results of the research work presented.

Table 3. Global properties of the adobe samples.

	Adobe Sample	Fibres %-L	$\rho$ [kg/m <sup>3</sup> ]	$\lambda$ [W/(mK)]	Fmax ( $\sigma_c$ ) [N]	$\sigma_c$ [MPa]	Fmax ( $\sigma_f$ ) [N]	$\sigma_f$ [MPa]
PHASE I	P0	-	1933.71	0.754				
PHASE II	P1	-	1741.33	0.546	2482.29	1.55	204.37	0.48
	P2	1%-1–3 cm	1431.33	0.529	1600.00	1.00	189.48	0.44
	P3	2%-1–3 cm	1542.33	0.298	1053.13	0.65	112.50	0.26
	P4	1%-3–6 cm	1445.33	0.550	1145.83	0.71	182.50	0.42
	P5	2%-3–6 cm	1546.67	0.453	982.29	0.59	143.64	0.33
	P6	3%-3–6 cm	1279.00	0.298	1315.70	0.82	151.44	0.35
PHASE III	Correlation between the properties resulting from the above tests.							

During the initial stage of the investigation (Phase I), the adobe block extracted from an old adobe building representative of the building stock of the village of Torres, Anadia was evaluated to create a product that mirrors the physical, chemical, and mechanical attributes of the original adobe as closely as possible. First, the adobe mixture was evaluated, based on the grain size curve acquired from the original adobe block. This process is crucial for any subsequent restoration intervention seeking to safeguard the identity of a location using information on its soil.

In Phase II of the work, adobe bricks were tested on the basis of the grain size curve and mineralogical analysis obtained from the original P0 adobe, with different percentages of reinforcement of local bunho and junco plant fibres. The physical properties of the samples obtained were then tested. The thermal conductivity was determined to be 0.529–0.298 W/mK for P2–P3 with 1–2% of fibres measuring between 10 and 30 mm, and 0.550–0.453–0.298 W/mK for P4–P5–P6 with 1–2–3% of 10–30 mm fibres; the density increased with the addition of fibres, going from 1714 kg/m<sup>3</sup> without any addition to 1431–1445 kg/m<sup>3</sup> with 1% addition, 1542–1546 kg/m<sup>3</sup> with 2%. The water absorption test indicated that the incorporation of fibres enhances the resistance of adobe to capillary water. The results of the tested formulations can be classified as weakly capillary ( $C_b < 20$ ), with the best result being P2 with 1% of 10–30 mm fibres.

In Phase III, the effects of varying the length and percentage of vegetal fibre reinforcement on the properties of adobe samples were evaluated. The mechanical properties of adobe are affected by fibre content. An increase in fibre content leads to a decrease in compression. The compression test showed that the adobe block taken from the building

had a maximum compressive strength of  $\sigma_c \max = 5.86$  MPa; the compression tests on the P1\* species, without reinforcement, gave  $\sigma_c \max = 1.61$  MPa with a value closer to the compression test of the wet than the dry historical adobe, which could indicate that 28 days of curing is not sufficient. The flexure test, carried out only on adobe samples with fibres, shows, in the case of sample P5.3\_L3-6, that the 2% proportion of fibres of 30–60 mm length affects the material behaviour, giving it a diagonal curve.

Fibre length influences the results of the compression test: the addition of 2% smaller fibres and 1% larger fibres had the same effect on compressive strength. Young's modulus values were acceptable with the addition of 2% fibres.

There is no clear correlation between compression resistance and density of adobe with fibres. However, various studies suggest a reduction in thermal conductivity that follows a parabolic or linear regression as the density decreases [60,77]. Previous research [74] suggests a flawless connection between compressive strength and density and a strong linear relationship between thermal conductivity and adobe density. Several studies suggest a reduction in thermal conductivity that follows a parabolic or linear regression as density decreases; this was also demonstrated in our research. Furthermore, a linear regression emerged with the addition of fibres 1–3 cm in length and a parabolic regression with the addition of fibres 3–6 cm.

## 6. Conclusions

The research proposes the utilisation of fibres derived from local bunho and junco plants as a means of producing adobe blocks. The objective is to utilise these blocks for the renovation and reconstruction of adobe buildings in the central region of Portugal, where adobe is the predominant technique. To undertake the requisite safeguarding actions, it is first necessary to have a detailed understanding of the properties of the built stock. Consequently, the characterisation of adobe blocks was carried out for a typological unit in Anadia (PT), in the village of Torres. The built heritage in the municipality is recognised by the historical villages of Portugal but has not yet been the subject of scientific research.

The results of the mineralogical and particle size analyses were used to recreate the soil, thereby initiating the production of fibre-reinforced adobe samples. These samples were composed of local bunho and junco fibres sourced from the wetland area of the same village, with varying percentages and reinforcement lengths.

The utilisation of fibres derived from wetland flora serves to promote biodiversity, given that these plants exhibit rapid growth and are considered weedy.

From the characterisations, it can be concluded that the P3 and P6 fibre samples possess insulating properties. Consequently, an increase in the percentage of reinforcement in the adobe contributes to enhanced insulation. The length of the fibres has an impact on the results of the compression test, with adobe samples comprising 2% fibres of lengths between 10 and 30 mm and 1% fibres of lengths between 30 and 40 mm.

Moreover, the blocks produced demonstrate potential applications in the energy retrofitting of existing adobe buildings and the construction of new nZEB buildings, thereby contributing to the preservation of this traditional building technique. Indeed, the results demonstrate that the production of the adobe we have developed and tested has the potential to contribute to the creation of new sources of sustainable and circular economic activity in these rural areas, which are recognised as heritage sites that require protection from the risk of depopulation. This can be achieved by stimulating the necessary building maintenance and recovery operations for this heritage to be usable for future generations, while also contributing to the resilience of the village.

**Author Contributions:** Conceptualisation, A.R. and R.V.; methodology, A.R.; software, A.R.; validation, A.R., R.V., V.F. and H.R.; formal analysis, A.R., R.V., H.R. and V.F.; investigation, A.R.; resources, A.R.; data curation, A.R.; writing—original draft preparation, A.R.; writing—review and editing, A.R., R.V., V.F. and H.R.; visualisation, R.V.; supervision, R.V. All authors have read and agreed to the published version of the manuscript.

**Funding:** This research did not receive any external funding.

**Data Availability Statement:** The data presented in this study are available on request from the corresponding author.

**Acknowledgments:** The University of Naples Federico II (IT) financed the research period of the XXXVII PhD cycle at the Department of Civil Engineering of the University of Aveiro (PT).

**Conflicts of Interest:** The authors declare that they have no conflicts of interest. The graphs, images, and writing are by doctoral candidate Angelica Rocco, who was supervised in applying the methodology and reviewing the work prepared by the other authors.

## Appendix A

**Table A1.** Mechanical properties of the adobe samples after 28 days. P1\* sample produced compared with the results of chemical and mineralogical analysis of the adobe brick sample taken from the building under study. \*\* The test did not give the result even when repeated 2 times in a row.

Adobe Sample	Acronym	Fibres %	Fmax ( $\sigma_c$ ) [N]	$\sigma_c$ [MPa]	Fmax ( $\sigma_f$ ) [N]	$\sigma_f$ [MPa]
P1*	P1.1	0	2375.00	1.48	189.06	0.44
	P1.2		2484.38	1.55	219.06	0.51
	P1.3		2587.50	1.61	205	0.48
	Average		2482.29	1.55	204.37	0.48
Stand. Dev.			106.26	0.06	15.01	0.03
			0.04	0.04	0.07	0.07
	Variation					
P2	P2.1_L1-3	1	1725.00	1.07	225.00	0.52
	P2.2_L1-3		164.63	1.02	172.50	0.40
	P2.3_L1-3		1434.38	0.89	170.94	0.40
	Media		1600.00	1.00	189.48	0.44
Stand. Dev.			149.51	0.09	30.77	0.07
			0.09	0.09	1.16	0.16
	Variation					
P3	P3.1_L1-3	2	921.87	0.57	152.18	0.35
	P3.2_L1-3		1131.25	0.70	111.87	0.26
	P3.3_L1-3		1106.25	0.69	73.43	0.17
	Media		1053.13	0.65	112.50	0.26
Stand. Dev.			114.35	0.071	39.37	0.09
			0.11	0.11	0.35	0.35
	Variation					
P4	P4.1_L3-6	1	1068.75	0.66	176.87	0.41
	P4.2_L3-6		1187.50	0.74	185.94	0.43
	P4.3_L3-6		1181.25	0.73	184.68	0.43
	Media		1145.83	0.71	182.50	0.42
Stand. Dev.			66.83	0.04	4.91	0.01
			0.058	0.06	0.02	0.027
	Variation					
P5	P5.1_L3-6	2	1034.38	0.64	129.37	0.30
	P5.2_L3-6		1040.63	0.65	179.68	0.42
	P5.3_L3-6 **		871.87	0.54	121.87	0.28
	Media		982.29	0.59	143.64	0.33
Stand. Dev.			95.67	0.09	31.43	0.07
			0.09	0.09	0.21	0.21
	Variation					
P6	P6.1_L3-6	3	568.75	0.35	79.37	0.18
	P6.2_L3-6		746.87	0.46	79.68	0.18
	P6.3_L3-6		576.25	0.47	69.37	0.16
	Media		690.62	0.43	76.14	0.17
Stand. Dev.			105.65	0.06	5.86	0.01
			0.15	0.15	0.07	0.07
	Variation					
Media			1315.70	0.82	151.44	0.35
	Stand. Dev.		607.09	0.37	51.40	0.12
	Variation		0.45	0.45	0.34	0.34

## References

1. International Energy Agency. Available online: <http://www.iea.org/> (accessed on 20 July 2023).
2. Piaia, E.; Turillazzi, B.; Di Giulio, R.; Sebastian, R. Advancing the Decarbonization of the Construction Sector: Lifecycle Quality and Performance Assurance of Nearly Zero-Energy Buildings. *Sustainability* **2024**, *16*, 3687. [\[CrossRef\]](#)
3. MacDougall, C. Natural building materials in mainstream construction: Lessons from the UK. *J. Green Build.* **2008**, *3*, 1–14. [\[CrossRef\]](#)
4. Beckett, C.; Jaquin, P.A.; Morel, J.C. Weathering the storm: A framework to assess the resistance of earthen structures to water damage. *Constr. Build. Mater.* **2020**, *242*, 118098. [\[CrossRef\]](#)
5. Schroeder, H. *Sustainable Building with Earth*; Springer: Cham, Switzerland, 2016; Volume 582.
6. Moriset, S.; Rakotomamonjy, B.; Gandreau, D. Can earthen architectural heritage save us? *Built Herit.* **2021**, *5*, 19. [\[CrossRef\]](#)
7. Pinto, R. *Génese e Evolução dos Solos*; Universidade Técnica de Lisboa, Instituto Superior de Agronomia, Departamento de Ciências do Ambiente: Lisboa, Portugal, 1969; pp. 15–16.
8. Rua, M.H. *Os dez Livros de Arquitectura de Vitruvius*; Edição ICIST: Kaunas, Lithuania, 1998; pp. 535–538.
9. Adam, J.P.; Guidobaldi, M.P.; Torelli, M.; Torelli, M. *L'arte di Costruire Presso i Romani: Materiali e Tecniche*; Longanesi: Milan, Italy, 1988.
10. Motta, M. *Construções Rurais em Alvenaria de Terra Crua no Baixo Alentejo*; Universidade Técnica de Lisboa, Instituto Superior Técnico: Lisboa, Portugal, 1997.
11. Shukla, A.; Tiwari, G.N.; Sodha, M.S. Embodied energy analysis of adobe house. *Renew. Energy* **2009**, *34*, 755–761. [\[CrossRef\]](#)
12. Lima, J.; Faria, P.; Santos Silva, A. Earth plasters: The influence of clay mineralogy in the plasters' properties. *Int. J. Archit. Herit.* **2020**, *14*, 948–963. [\[CrossRef\]](#)
13. Fabbri, A.; McGregor, F.; Costa, I.; Faria, P. Correction to: Effect of temperature on the sorption curves of earthen materials. *Mater. Struct.* **2019**, *52*, 24. [\[CrossRef\]](#)
14. Silva, A.; Oliveira, I.; Silva, V.; Mirão, J.; Faria, P. Vernacular Caramel' s Adobe Masonry Dwellings–Material Characterization. *Int. J. Archit. Herit.* **2022**, *16*, 67–84. [\[CrossRef\]](#)
15. Sposito, S.; Scalisi, F. Sustainable architecture: The eco-efficiency earth construction. *Eur. J. Sustain. Dev.* **2017**, *6*, 246.
16. Olacia, E.; Pisello, A.L.; Chiodo, V.; Maisano, S.; Frazzica, A.; Cabeza, L.F. Sustainable adobe bricks with seagrass fibres. Mechanical and thermal properties characterization. *Constr. Build. Mater.* **2020**, *239*, 117669. [\[CrossRef\]](#)
17. Vijayan, D.S.; Nivetha, C.; Kumar, P.D.; Saravanan, B.; Gogulnath, V. Green composite form of eco-friendly concrete by adding PVA fiber. *J. Green Eng. (JGE)* **2020**, *10*, 3084–3101.
18. Papayianni, I.; Pacht, V. Earth block houses of historic centers. A sustainable upgrading with compatible repair materials. *Procedia Environ. Sci.* **2017**, *38*, 274–282. [\[CrossRef\]](#)
19. Rafi, M.M.; Varum, H. Seismic performance of adobe construction. *Sustain. Resilient Infrastruct.* **2017**, *2*, 8–21. [\[CrossRef\]](#)
20. Galindo, A.L.; Ruiz, J.T.; Lopez, J.G. Mineral quantification in sepiolite-palygorskite deposits using X-ray diffraction and chemical data. *Clay Miner.* **1996**, *31*, 217–224. [\[CrossRef\]](#)
21. Millogo, Y.; Hajjaji, M.; Ouedraogo, R. Microstructure and physical properties of lime-clayey adobe bricks. *Constr. Build. Mater.* **2008**, *22*, 2386–2392. [\[CrossRef\]](#)
22. Gokulnath, V.; Vijayan, D.S.; Kathirvel, P.; Karthikraja, S.; Saravanan, B. Behaviour of retro fitted beams using natural fibers. *Mater. Today Proc.* **2020**, *33*, 949–953. [\[CrossRef\]](#)
23. Millogo, Y.; Morel, J.C.; Aubert, J.E.; Ghavami, K. Experimental analysis of Pressed Adobe Blocks reinforced with Hibiscus cannabinus fibers. *Constr. Build. Mater.* **2014**, *52*, 71–78. [\[CrossRef\]](#)
24. Segetin, M.; Jayaraman, K.; Xu, X. Harakeke reinforcement of soil–cement building materials: Manufacturability and properties. *Build. Environ.* **2007**, *42*, 3066–3079. [\[CrossRef\]](#)
25. Regione Piemonte L.R. 2/06, Norme per la valorizzazione delle costruzioni in terra cruda. 2006. BUR Piemonte, 3. Available online: <https://www.gazzettaufficiale.it/atto/regioni/caricaDettaglioAtto/originario?atto.dataPubblicazioneGazzetta=2007-06-30&atto.codiceRedazionale=006R0449> (accessed on 28 July 2023).
26. Gazzetta Ufficiale Italiana, n. 378 Legge 24 Dicembre 2003, Disposizioni per la tutela e la valorizzazione dell'architettura rurale. 2004. Available online: [https://www.gazzettaufficiale.it/atto/serie\\_generale/caricaDettaglioAtto/originario?atto.dataPubblicazioneGazzetta=2004-01-17&atto.codiceRedazionale=004G0014&elenco30giorni=false](https://www.gazzettaufficiale.it/atto/serie_generale/caricaDettaglioAtto/originario?atto.dataPubblicazioneGazzetta=2004-01-17&atto.codiceRedazionale=004G0014&elenco30giorni=false) (accessed on 28 July 2023).
27. *New Mexico Earthen Building Materials Code*; GCB-NMBC-14.7.4 (2006); Regulation & Licensing Department, Construction Industries Division, Construction Industries Bureau: Santa Fe, NM, USA, 2006.
28. AS 4773.2-2015; Masonry in Small Buildings Construction. Standards Australia Limited: Sydney, Australia, 2015. Available online: <https://store.standards.org.au/product/as-4773-2-2015> (accessed on 28 July 2023).
29. AS 3700-2018; Masonry Structures. Standards Australia: Sydney, Australia, 2018. Available online: <https://wabuildinginspections.com.au/wp-content/uploads/AS3700%202018%20Masonry%20Structures.pdf> (accessed on 28 July 2023).
30. TS 2514; Production and Usage of Adobe Bricks. Turkish Standards Institution: Ankara, Türkiye, 1997.
31. Larsen, K.E. (Ed.) Nara Conference on Authenticity in relation to the World Heritage Convention, Nara, Japan, 1–6 November 1994. Available online: <https://whc.unesco.org/archive/nara94.htm> (accessed on 30 July 2023).
32. Saxton, R.H. Performance of cob as a building material. *Struct. Eng.* **1995**, *73*, 111–115.

33. Varum, H.; Costa, A.; Velosa, A.; Martins, T.; Pereira, H.; Almeida, J. Caracterização mecânica e patológica das construções em Adobe no distrito de Aveiro como suporte em intervenções de reabilitação. *Proj. Cult.* **2000**, 41–45. Available online: [https://ria.ua.pt/bitstream/10773/7799/1/I\\_027.pdf](https://ria.ua.pt/bitstream/10773/7799/1/I_027.pdf) (accessed on 28 June 2023).
34. Bruno, P.; Faria, P. Earth mortars use on neolithic domestic structures. Some case studies in Alentejo, Portugal. *Conserv. Património* **2008**, 5–12. Available online: <https://www.redalyc.org/pdf/5136/513653433002.pdf> (accessed on 2 July 2023).
35. García y Bellido, A. Orígenes de la casa redonda de la cultura castreña del NO de la Península. 1971. Available online: <https://www.castrosdeasturias.es/descargas/703-garcia-y-bellido-a.-1971.-revista-guimaraes-81-3-4-25-35.-origenes-casa-redonda-cultura-castrea-nw.pdf> (accessed on 2 July 2023).
36. Instituto Nacional de Estatística. Censos 2011. Available online: <https://censos.ine.pt/> (accessed on 28 June 2023).
37. Costa, C.; Arduin, D.; Rocha, F.; Velosa, A. Adobe blocks in the center of Portugal: Main characteristics. *Int. J. Archit. Herit.* **2021**, 15, 467–478. [CrossRef]
38. Fernandes, M. *O adobe e as alvenarias de adobe em Portugal. erra em Seminário*; Argumentum: Aveiro, Portugal, 2007; pp. 116–119.
39. Dias, J. O problema da reconstituição das casas redondas castrejas. In *Trabalhos de Antropologia e Etnologia*; Instituto De Antropologia, Faculdade de Ciências: Porto, Portugal, 1948; Volume 12. Available online: <https://ojs.letras.up.pt/index.php/tae/article/view/8572/7849> (accessed on 13 July 2023).
40. Correia, M.; Carlos, G.; Rocha, S. (Eds.) *Vernacular Heritage and Earthen Architecture*; CRC Press: London, UK, 2013. [CrossRef]
41. Silveira, D.; Varum, H.; Costa, A.; Lima, E. Levantamento e caracterização do parque edificado em adobe na cidade de Aveiro. digitAR-Revista Digital de Arqueologia. *Arquit. Artes* **2013**. [CrossRef]
42. Tavares, A.; Costa, A.; Varum, H. Adobe and modernism in Ílhavo, Portugal. *Int. J. Archit. Herit.* **2012**, 6, 525–541. [CrossRef]
43. da Silveira, D.S.G. Constructive and Mechanical Characterisation of Adobe Masonry Walls of Existing Buildings. Doctoral Dissertation, Universidade de Aveiro, Aveiro, Portugal, 2016.
44. da Costa, A.M.T.A. Integrated Conservation Strategy of Built Heritage. Doctoral Dissertation, Universidade de Aveiro, Aveiro, Portugal, 2015.
45. Costa, C.; Cerqueira, Â.; Rocha, F.; Velosa, A. The sustainability of adobe construction: Past to future. *Int. J. Archit. Herit.* **2018**, 13, 639–647. [CrossRef]
46. Formisano, A.; Chiumiento, G. Physical-Mechanical Experimental Tests on Adobe Bricks Reinforced with Hemp Fibres. *J. Archit. Constr.* **2018**, 1, 25–36.
47. Ouedraogo, M.; Dao, K.; Millogo, Y.; Aubert, J.E.; Messan, A.; Seynou, M.; Zerbo, L.; Gomina, M. Physical, thermal and mechanical properties of adobes stabilized with fonio (*Digitaria exilis*) straw. *J. Build. Eng.* **2019**, 23, 250–258. [CrossRef]
48. Babé, C.; Kidmo, D.K.; Tom, A.; Mvondo, R.R.N.; Boum, R.B.E.; Djongyang, N. Thermomechanical characterization and durability of adobes reinforced with millet waste fibers (*sorghum bicolor*). *Case Stud. Constr. Mater.* **2020**, 13, e00422. [CrossRef]
49. Ramakrishnan, S.; Loganayagan, S.; Kowshika, G.; Ramprakash, C.; Aruneshwaran, M. Adobe blocks reinforced with natural fibres: A review. *Mater. Today Proc.* **2021**, 45, 6493–6499. [CrossRef]
50. Kim, C.; Shin, H.; Choi, H.K. A phenetic analysis of *Typha* in Korea and far east Russia. *Aquat. Bot.* **2003**, 75, 33–43. [CrossRef]
51. Müller-Sämann, K.M.; Reinhardt, G.; Vetter, R.; Gärtner, S. Nachwachsende Rohstoffe in Baden-Württemberg: Identifizierung vorteilhafter Produktlinien zur stofflichen Nutzung unter besonderer Berücksichtigung umweltgerechter Anbauverfahren. Projektabschluss-bericht Forschungszentrum Karlsruhe IfUL Müllheim. 2003. Available online: [https://pudi.lubw.de/detailseite/-/publication/28764-Nachwachsende\\_Rohstoffe\\_in\\_Baden-W%C3%BCrttemberg\\_Identifizierung\\_vorteilhafter\\_Produktlinien\\_zur\\_stoffl.pdf](https://pudi.lubw.de/detailseite/-/publication/28764-Nachwachsende_Rohstoffe_in_Baden-W%C3%BCrttemberg_Identifizierung_vorteilhafter_Produktlinien_zur_stoffl.pdf) (accessed on 20 July 2023).
52. Niang, I.; Maalouf, C.; Moussa, T.; Bliard, C.; Samin, E.; Thomachot-Schneider, C.; Lachi, M.; Pron, H.; Mai, T.H.; Gaye, S. Hygrothermal performance of various *Typha*–clay composite. *J. Build. Phys.* **2018**, 42, 316–335. [CrossRef]
53. ISO 2597-2:2019; Iron Ores—Determination of Total Iron Content. International Organization for Standardization: Geneva, Switzerland, 2017.
54. ISO 12677:2011; Chemical Analysis of Refractory Products by X-ray Fluorescence (XRF)—Fused Cast-Bead Method. International Organization for Standardization: Geneva, Switzerland, 2011.
55. ISO 8301:1991; Thermal Insulation—Determination of Steady-State Thermal Resistance and Related Properties—Heat Flow Meter Apparatus. International Organization for Standardization: Geneva, Switzerland, 1991.
56. CEN EN 933-1:2012; Tests for Geometrical Properties of Aggregates—Part 1: Determination of Particle Size Distribution—Sieving Method. European Committee for Standardization: Brussels, Belgium, 2012.
57. UNI 9944:1992; Corrosion and Protection of Concrete Reinforcement. Determination of Carbonation Depth and Chloride Ion Penetration Profile in Concrete. Italian Standards Authority: Milan, Italy, 1992.
58. UNI EN 15801:2010; Conservation of Cultural Property—Test Methods—Determination of Water Absorption by Capillarity. Italian Standards Authority: Milan, Italy, 2010.
59. EN:1015-11; Methods of Test for Mortar for Masonry—Part 11: Determination of Flexural and Compressive Strength of Hardened Mortar. European Committee for Standardization: Brussels, Belgium, 2020.
60. ISO 17025:2017; General Requirements for the Competence of Testing and Calibration Laboratories. International Organization for Standardization: Geneva, Switzerland, 2017.
61. Comina, C.; Lancellotta, R.; Foti, S.; Musso, G. Tomografie elettriche su campioni di laboratorio. In Proceedings of the IARG Incontro Annuale dei Ricercatori di Geotecnica, Trento, Italy, 7–9 July 2004.



62. BS EN 932-2; Tests for General Properties of Aggregates, Part 2: Methods for Reducing Laboratory Samples. British Standard Institution: London, UK, 1999.
63. Quagliarini, E.; Lenci, S. The influence of natural stabilizers and natural fibres on the mechanical properties of ancient Roman adobe bricks. *J. Cult. Herit.* **2010**, *11*, 309–314. [\[CrossRef\]](#)
64. Diatta, M.T.; Gaye, S.; Thiam, A.; Azilinson, D. Détermination des propriétés thermo-physique et mécanique du typha australis. In Proceedings of the Congres SFT, Perpignan, France, 24–27 May 2011.
65. Dieye, Y.; Sambou, V.; Faye, M.; Thiam, A.; Adj, M.; Azilinson, D. Thermo-mechanical characterization of a building material based on Typha Australis. *J. Build. Eng.* **2017**, *9*, 142–146. [\[CrossRef\]](#)
66. Maddison, M.; Mauring, T.; Kirsimäe, K.; Mander, Ü. The humidity buffer capacity of clay–sand plaster filled with phytomass from treatment wetlands. *Build. Environ.* **2009**, *44*, 1864–1868. [\[CrossRef\]](#)
67. Ba, L.; El Abbassi, I.; Ngo, T.T.; Pliya, P.; Kane CS, E.; Darcherif, A.M.; Ndongo, M. Investigation of the length and percentage fiber influence of Typha Australis on biosourced composites. In Proceedings of the E3S Web of Conferences, Pekanbaru, Indonesia, 26 November 2021; EDP Sciences: Les Ulis, France, 2022; Volume 353, p. 01002.
68. Achenza, M.; Atzeni, C.; Mocci, S.; Sanna, U. *Il Manuale Tematico della Terra Cruda: Caratteri, Tecnologia, Buone Pratiche*; Dei S.r.l.-Tipografia del Genio Civile: Milan, Italy, 2008. Available online: <https://www.sardegna.digitallibrary.it/mmt/fullsize/2009022319494200003.pdf> (accessed on 2 June 2023).
69. Adobes! Porque não? Integração do adobe como processo construtivo na arquitetura contemporânea. 2017. Available online: <https://repositorio-aberto.up.pt/handle/10216/121163> (accessed on 2 June 2023).
70. EN 196-1:2005; Methods of Testing Cement—Part 1: Determination of Strength. European Committee for Standardization: Brussels, Belgium, 2005.
71. BS EN 14630:2006; Products and Systems for the Protection and Repair of Concrete Structures—Test Methods—Determination of Carbonation Depth in Hardened Concrete by the Phenolphthalein Method. European Standard: Brussels, Belgium, 2007.
72. RRUFF Sample Data. Database. Available online: <https://rruff.info/al/display=default/> (accessed on 1 September 2023).
73. Costa, L.R.R. Caracterização Física, Mineralógica e Mecânica de Adobes de Aveiro. Doctoral Dissertation, Universidade de Aveiro, Aveiro, Portugal, 2014.
74. Capitolo 8: Chimica applicata, in *Manuale prove e sperimentazioni*. Istituto Sperimentale per l’Edilizia. 2002. Available online: <https://istedil.it/manuale-prove-e-sperimentazioni> (accessed on 18 September 2023).
75. Charai, M.; Salhi, M.; Horma, O.; Mezrhab, A.; Karkri, M.; Amraoui, S. Thermal and mechanical characterization of adobes bio-sourced with Pennisetum setaceum fibers and an application for modern buildings. *Constr. Build. Mater.* **2022**, *326*, 126809. [\[CrossRef\]](#)
76. Danso, H.; Martinson, D.B.; Ali, M.; Williams, J.B. Physical, mechanical and durability properties of soil building blocks reinforced with natural fibres. *Constr. Build. Mater.* **2015**, *101*, 797–809. [\[CrossRef\]](#)
77. Khoudja, D.; Taallah, B.; Izemmouren, O.; Aggoun, S.; Herihiri, O.; Guettala, A. Mechanical and thermophysical properties of raw earth bricks incorporating date palm waste. *Constr. Build. Mater.* **2021**, *270*, 121824. [\[CrossRef\]](#)

**Disclaimer/Publisher’s Note:** The statements, opinions and data contained in all publications are solely those of the individual author(s) and contributor(s) and not of MDPI and/or the editor(s). MDPI and/or the editor(s) disclaim responsibility for any injury to people or property resulting from any ideas, methods, instructions or products referred to in the content.